The present study on *C. versicolor* revealed that there is no relationship between internalized yolk mass and maternal body size and mass, and clutch mass, but is significantly influenced by breeding time through the egg mass. The internalized yolk mass that is significantly more in hatchlings born in the late breeding season is correlated with their egg mass. Interestingly, the heavier eggs in the later part of the breeding season did not produce large-sized hatchlings in terms of SVL compared to those arising from the smaller eggs of early clutches. Instead, there was an increase in the body mass as well as the amount of internalized yolk in hatchlings born in the late breeding season. In reptiles, hatchling size alone is not an important correlate of hatchling survivorship, but internalized yolk is also a component of fitness for species whose hatchlings have to face competition for food and adverse environmental conditions like winter. Therefore, production of similar sized (SVL) hatchlings with greater body mass and residual yolk is beneficial for immediate post-hatching activity and survival[3]. The hatchlings of *C. versicolor* born later in the season may have to compete with the larger conspecific hatchlings of earlier clutches. Therefore, maximizing post-hatching energy through internalized yolk in the later part of the breeding season may indeed outweigh the advantages, if any, of maximizing the linear body size. Hence, in *C. versicolor*, selection has favoured greater amount of body mass and residual yolk to enhance fitness of late-born hatchlings.

1. Burghardt, G. M., *Am. Zool.*, 1977, **17**, 177–190.
2. Kraemer, J. E. and Bennett, S. H., *Copeia*, 1981, **1981**, 406–411.
3. Packard, G. C., in *Egg Incubation: Its Effects on Embryonic Development in Birds and Reptiles* (eds Deeming, D. C. and Ferguson, M. W.), Cambridge University Press, New York, 1991, pp. 213–228.
4. Wilhoft, D. C., *Comp. Biochem. Physiol.*, 1996, **84A**, 483–486.
5. Troyer, K., *Oecologia*, 1983, **58**, 340–344.
6. Tucker, J. K., Filoramo, N. I., Paukstis, G. L. and Janzen, F. J., *Copeia*, 1998, **1998**, 488–492.
7. Shanbhag, B. A. and Prasad, B. S. K., *J. Morphol.*, 1993, **216**, 1–7.
8. Shanbhag, B. A., Radder, R. S. and Saidapur, S. K., *Copeia*, 2000, **2000**, 1062–1067.
9. Radder, R. S., Shanbhag, B. A. and Saidapur, S. K., *Amphibia-Reptilia*, 2002, **23**, 71–82.

ACKNOWLEDGEMENTS. This work is supported by a DST project (SP/SO/C-16/96) awarded to B.A.S. and partly supported by a grant from UGC SAP-II. R.S.R. was a Junior Research Fellow in the DST project.

Received 8 March 2002; revised accepted 16 April 2002

# Fractal dimension and *b*-value mapping in northeast India

**Pankaj Mala Bhattacharya[†,#], R. K. Majumdar* and J. R. Kayal[†]**

[†]Central Geophysics Division, Geological Survey of India, 27, Chowringhee Road, Kolkata 700 016, India
*Department of Geological Sciences, Jadavpur University, Kolkata 700 032, India

**The statistical characteristics of seismicity, fractal dimension and *b*-values are mapped in the NE India region using permanent microearthquake network data and teleseismic data. The maps revealed the seismogenic structures and the crustal heterogeneities, which are useful for earthquake risk evaluation.**

NORTHEAST India and adjacent areas are highly vulnerable to earthquake hazards. Any realistic seismic hazard assessment requires identification of seismic sources, evaluation of seismic characteristics with space and time, and frequency–magnitude relation for individual tectonic zones governed by the characteristics of faults.

Magnitude of an earthquake is the most commonly used parameter of earthquake size. The statistical distribution of sizes, for a group of earthquakes, is very complicated. Gutenberg and Richter[1] have provided a simplest earthquake reoccurrence or magnitude–frequency relation as $\log_{10}N = a - bM$, where $N$ is the number of earthquakes in the group having magnitudes larger than $M$, $a$ and $b$ are constants. The estimated coefficient $b$ known as the $b$-value, varies mostly from 0.7 to 1.3, depending on the tectonics of the region. The variability of $b$-values in different regions may be related to structural heterogeneity and stress distribution in space[2–4]. The $b$-value represents a statistical measurement of the relative abundance of large and small earthquakes in the group. A higher $b$-value means that a smaller fraction of the total earthquakes occur at the higher magnitudes, whereas a lower $b$-value implies a larger fraction occur at higher magnitudes. The higher levels of motion at a site are dominated by occurrences of the larger earthquakes. If $b$ is large, large earthquakes are relatively rare. It has been observed that the $b$-value shows systemic variations in the period preceding a major earthquake[5–7]. Hence it is the most investigated equation in seismology, observationally as well as theoretically. It has wide applications, e.g. for estimating the magnitude of future earthquakes, and to perform probabilistic hazard analysis.

The earthquake phenomenon possesses fractal structure with respect to time, space and magnitude. The Gutenberg–Richter[1] relation for frequency vs magnitude is a power law involving magnitude. Similarly, the after-

[#]For correspondence. (e-mail: gsicgd@cal2.vsnl.net.in)

shock decay follows another power law involving time[8]. The two-point spatial correlation function for earthquake epicentres also displays a power law structure[9]. Hence earthquakes are represented by self-similar mathematical construct, the 'fractal', and the scaling parameter is called the fractal dimension $D$[10]. It is a powerful tool to characterize the geometry that has a self-similar structure.

The fractal dimension of the spatial distribution of hypocentres may be related to the heterogeneity of the fractured material. The variability of the fractal dimension in different zones may be related to geological heterogeneity[11]. Fractal dimension gives vital information about the stability of a region. A change in fractal dimension corresponds to the dynamic evolution of the states of the system. It is scale-invariant and has introduced an efficient statistical parameter to quantify the dimensional distribution of seismicity and with that the proportion of randomness and clusterization[9,12,13]. Hirata[12] reported temporal variations in fractal dimension to quantify the seismic process, and Shimazaki and Nagahama[14] demonstrated that active fault systems in Japan possess self-similarity with fractal dimensions of 0.5 to 1.6. The fractal dimension characterizes the degree to which the fractal fills up the surrounding space. We can predict the fracture characteristic by knowing the value of $D$. A value of $D$ close to 3 implies that earthquake fractures are filling up a volume of the crust, a value close to 2 suggests that it is a plane that is being filled up, and a value close to 1 means that line sources are predominant[15]. Tosi[16] illustrated that possible values of fractal dimension are bound to range between 0 and 2, which is dependent on the dimension of the embedding space. Interpretation of such limit values is that a set with $D \to 0$ has all events clustered into one point, and at the other end of the scale, $D \to 2$ indicates that the events are randomly or homogeneously distributed over a two-dimensional embedding space.

In this communication, an attempt has been made to map the spatial distribution of $D$ and $b$-value in northeast India which is one of the most seismically active regions in the world. The teleseismic data of the *International Seismological Catalogue* (ISC) and the telemetric microearthquake network data of the National Geophysical Research Institute (NGRI) and Regional Research Laboratory, Jorhat (RRL(J)) bulletins are used in this investigation. Results of this study are discussed in terms of seismotectonics of the region.

Northeast India and the adjoining areas, latitude 24–28°N and longitude 89–98°E, fall in one of the most intense seismic zones of the world. It has been the seat of two great earthquakes ($M > 8.0$); the 1897 great Shillong

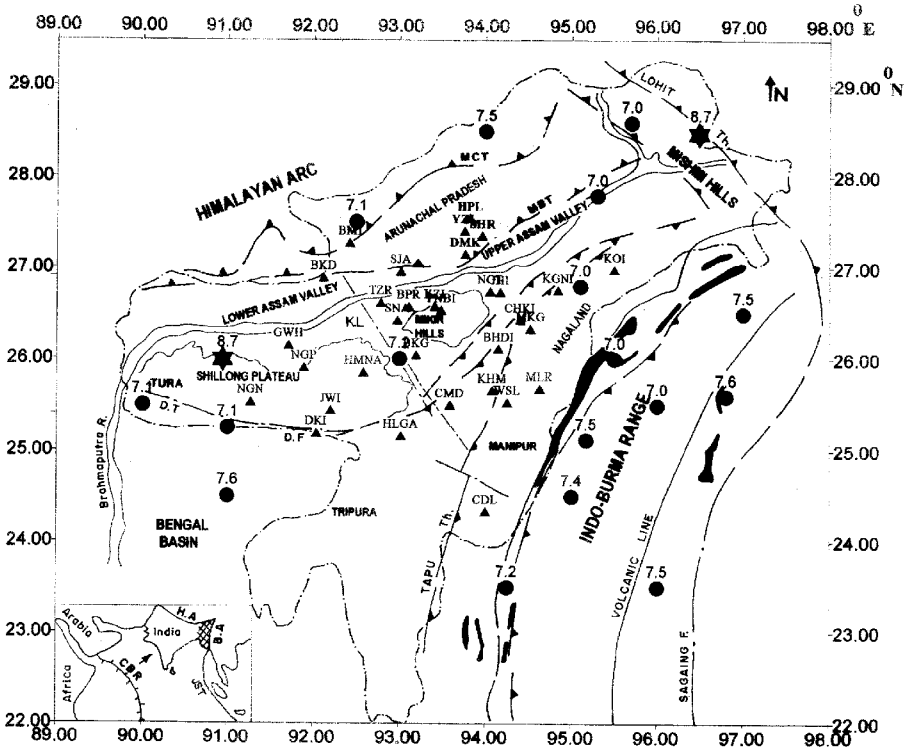


**Figure 1.** Map showing epicentres of large earthquakes ($M \geq 7.0$) in the region; the two great earthquakes ($M > 8.0$) are shown as star symbols. The permanent seismic stations are shown by solid triangles. MCT, Main Central Thrust; MBT, Main Boundary Thrust; DF, Dauki Fault; DT, Dapsi Thrust; KL, Kopili Lineament. (Inset) Key map of the study area, HA, Himalayan Arc; BA, Burmese Arc; CBR, Carls Berg Ridge.

earthquake ($M$ 8.7) and the 1950 great Assam earthquake ($M$ 8.7), with catastrophic damage to life and property in the region. The region displays tectonically distinct geological domains occurring in intimate spatial association (Figure 1). The Himalayan arc binds the region to the north and the Burmese arc to the east. The earthquakes in the Himalayan arc are referred to collision tectonics and are correlated with the known regional thrusts, the Main Boundary Thrust (MBT) and the Main Central Thrust (MCT) (Figure 1). The earthquakes are confined within a depth of 80 km (ref. 17). Thrust faulting is reported for the teleseismic earthquakes in the Himalayan arc[18]. Microearthquake investigation, however, revealed transverse tectonics in the Arunachal Himalaya[19]. The earthquakes in the Burmese arc, on the other hand, are referred to subduction tectonics; normal, thrust and strike-slip faulting are reported[17,20–22]. The earthquakes are as deep as 200 km. The meeting zone of the Himalayan arc and the Burmese arc, the Assam syntaxis, is also seismically active and was the source of the 1950 great Assam–Tibet earthquake ($M$ 8.7). The Shillong Plateau and Assam valley area, bounded by the MBT to the north and by the Dauki Fault to the south, are well known for their high seismic activity and produced the 1897 great Shillong earthquake ($M$ 8.7). The earthquakes in the plateau region are mostly confined within a depth of 35 km; reverse faulting and strike-slip faulting earthquakes are reported in the plateau region[23]. To the east of the Shillong Plateau lies the Mikir massif, which is separated from the Shillong massif by a NW–SE major lineament/fault, called the Kopili Lineament[24]. The Mikir Hills area is equally active as the Shillong Plateau area[23].

Since the inception of the Worldwide Seismograph Station Network (WWSSN) in 1964, it is observed that all the earthquakes of magnitudes $m_b > 4.5$ are more or less uniformly recorded in the study region. About 500 events were available for the period 1964–1993; the epicentre map is shown in Figure 2 *a*. In order to spatially map *b* and fractal dimension, the study area was grided at 2° spacing with an overlapping of 1°.

The permanent microearthquake data are published by the NGRI/RRL(J) in the form of bulletins. We have used five years (1993–1997) data with magnitude $M > 3.0$. We selected the threshold value of magnitude 3.0, so as to obtain a more reliable data set free from observation bias[25]. The data were grided at 2° and 1° spacing with an overlapping of 1° and 0.5° respectively. The 2° grid was studied for direct comparison of the map with that of the ISC data. About 800 well-located events were selected; the epicentre map is shown in Figure 2 *b*.

Smith[26] suggested the minimum number of points or events required for a reliable calculation of a correlation dimension as:

$$N_{\min} \geq \{R(2-Q)/r(1-Q)\}^{\mu},$$

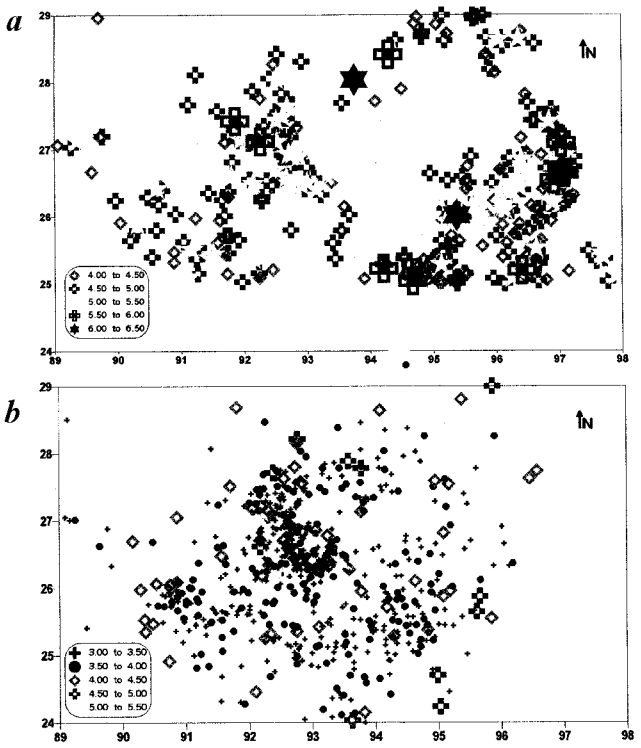


**Figure 2.** Map showing the epicentres of the selected events: ***a***, RRL(J) bulletin data; and ***b***, ISC data.

where $Q$ is a quality factor and $0 < Q < 1$, $R = r_{\max}/r_{\min}$, where $r$ is a scale to calculate $C_r$, $\mu$ is the greatest integer, less than the obtained fractal dimension of the set. The smallest topological dimension for the phase space in which the distribution of epicentres embeds is 2; therefore the value of $D$ will be less than 2, and hence $\mu = 1$. If $Q = 0.95$ and $r = 4$, we will have $N_{\min} > 42$. The number of events obtained from the ISC varies from 37 to 147 per grid, and that from the NGRI and RRL (J) bulletins, 74 to 291 per grid. This meets the condition for reliable calculations, expecting only few grids for the ISC data.

The events in each grid were used as a data set for analysis. These grids were interactively created, and seismically inactive area was excluded. Taking the centre of the grid as the plotting point, contour maps were prepared separately for *b*-value and fractal dimension.

In this study, the fractal dimension, the $D$ values, are estimated using the correlation dimension. The correlation dimension, as defined by Grassberger and Procaccia[27], measures the spacing of a set of points, which in this case are the earthquake epicentres. In principle, the fractal dimension of the hypocentre could be calculated avoiding the possible introduction of bias due to projection errors, but since the depths of earthquakes are much less well-determined than the horizontal position, it was deemed preferable to use the epicentres.

The correlation integral technique gives the correlation dimension; it is preferred to the box-counting algorithm, which gives a fractal 'capacity dimension' because of its greater reliability and sensitivity to small changes in clustering properties[9,12]. The correlation integral given by Grassberger and Procaccia[27] is:

$$D_{wr} = \lim_{r \to 0} \log(C_r)/\log r,$$

where $(C_r)$ is the correlation function. The correlation function measures the spacing or clustering of a set of points and is given by the relation:

$$C(r) = \frac{2}{N(N-1)} N(R < r),$$

where $N$ $(R < r)$ is the number of pairs $(X_i, X_j)$ with a smaller distance than $r$. The correlation integral is related to the standard correlation function as given by Kagan and Knopoff[9]:

$$C(r) \sim r^{D_2},$$

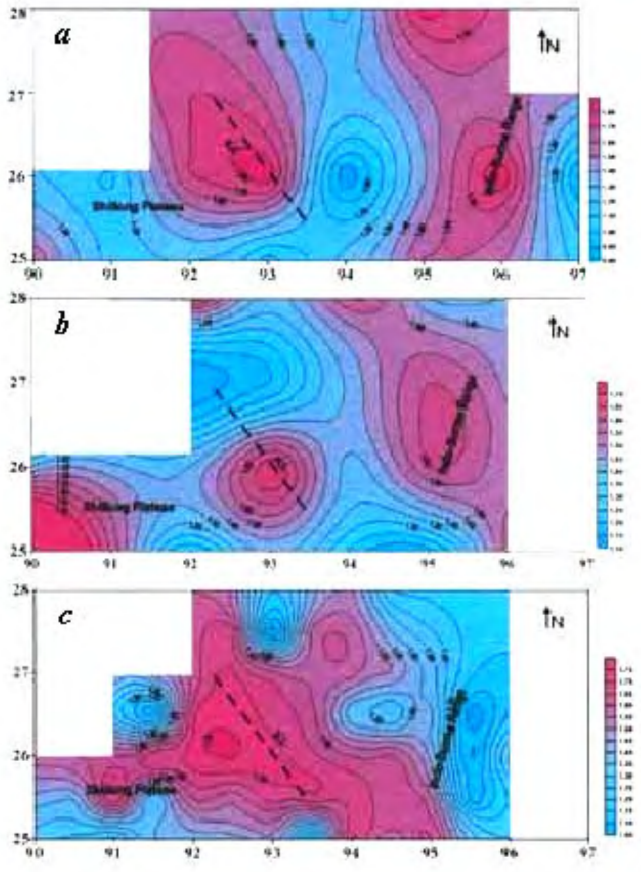


**Figure 3.** Map showing the contours of fractal dimension ($D$) in the study region: ***a***, ISC data with 2° grid; ***b***, NGRI/RRL(J) data with 2° grid, and ***c***, NGRI/RRL(J) data with 1° grid.

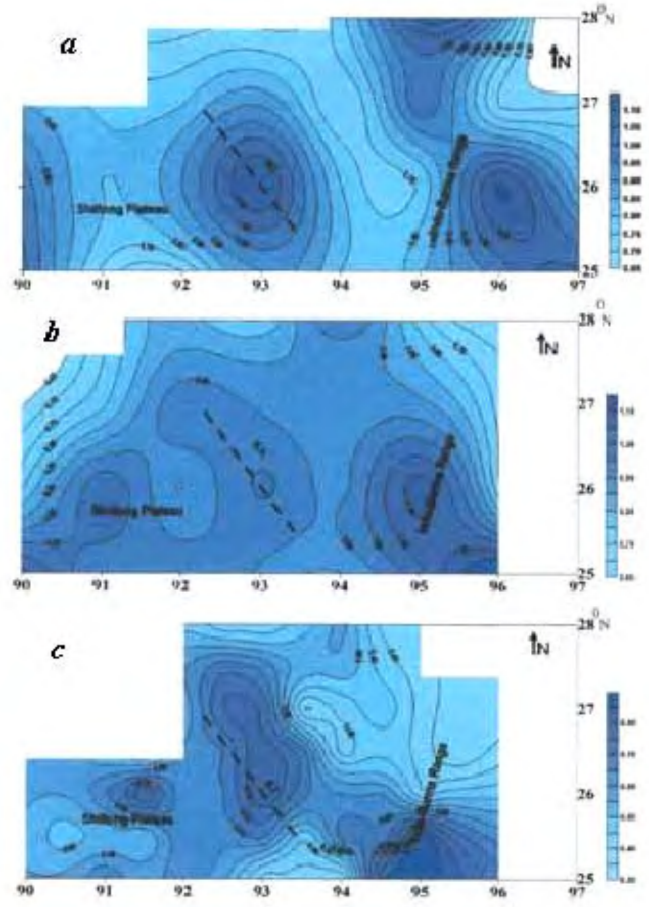


**Figure 4.** Map showing the contours of $b$-values for the earthquakes in the study region: ***a***, ISC data with 2° grid; ***b***, NGRI/RRL(J) data with 2° grid, and ***c***, RRL(J) data with 1° grid.

where $D_2$ is a fractal dimension, more strictly, the correlation dimension[27].

In this paper $D$ is used instead of $D_2$ for representing fractal dimension. Using this relation the $D$ value of spatial distribution of the earthquakes has been calculated, and the maps are prepared (Figure 3). A contour interval of 0.05 has been selected on the basis of error estimation. The sampling error is estimated using the sampling distribution theory. For all the three contour maps in Figure 3, error is found to vary from 0.02 to 0.03. Hence the contour interval of 0.05 is within the permissible limits. The value of 'test statistics' or '$Z$-score' is found to lie between 1.76 and 1.90, which is in the critical region $-1.96 \le Z \le 1.96$. This falls in 5% level of significance. Hence the level of confidence is 95%.

The $b$-value is calculated by the maximum likelihood method using the following equation given by Aki[28], which is based on theoretical considerations and is the most accepted method of $b$-value estimate:

$$b = \frac{\log e}{\overline{M} - M_0},$$

where $\overline{M}$ is the average magnitude and $M_0$ is the lower limit or threshold magnitude. The $b$-value estimate in each grid is used for preparing the map (Figure 4).

The study region, between longitudes 89°–98°E and latitudes 24°–29°N, exhibits tectonically distinct geological domains in intimate spatial association. Two epicentre maps are prepared; one from the ISC data ($M$ 4.0–6.5) for the period 1964–1993, and the other from the local permanent network data ($M$ 3.0–5.5) for the period 1993–97. The two epicentre maps are comparable. It is observed that seismicity along the Indo-Burma ranges in the subduction zone is very prominent. An intense activity is observed along the NW–SE Kopili Fault/Lineament. The next pronounced active zone is the Shillong Plateau.

The $b$-value maps (Figure 4 *a*–*c*) clearly depict the spatial variation of earthquake frequency in the region. Figure 4 shows higher $b$-value contours in the Indo-Burma ranges as well as in the Kopili Fault, and lower contours in the upper Assam valley area. The Shillong Plateau also shows a higher $b$-value contour. The NW–SE trend of higher $b$-value along the Kopili Fault extends from the Mikir Hills to Arunachal Himalaya across the MBT. The Indo-Burma ranges also show a NW–SE trend of higher $b$-value contour; and it extends in the dip direction of the subducted plate. These trends are maintained in all the three maps (Figure 4 *a*–*c*).

The $b$-value estimates from the ISC data and from the NGRI/RRL(J) data are comparable in 2° mapping (Figure 4 *a* and *b*), but the estimate in 1° mapping with the permanent network data is found to be comparatively lower. It may be noted here that the high $b$-value contours in Shillong Plateau are more distinct in Figure 4 *c*. Smaller grid size with sufficient number of events may be more effective in delineating the feature.

The variations in fractal dimension $D$ (Figure 3 *a*–*c*) values are comparable to those from some recent analysis[12,29,30]. According to Hirata[12], 1.6 is an upper limit to the fractal dimension of the fracture geometry that can be explained by the Griffith energy balance concept. The estimated fractal dimensions (1.10–1.85) in this study suggest that the faults are spatially distributed in the whole region, and the whole region is seismically active. In 2° mapping, the fractal dimension contours show a higher trend in the NW–SE direction along the Kopili lineament and along the Indo-Burma ranges (Figure 3 *a* and *b*), which are comparable with the higher $b$-value trends (Figure 4 *a* and *b*). The higher $D$ values in the Kopili Lineament (1.65–1.85) indicate more heterogeneity, possibly due to the deep-rooted Kopili Fault, a transverse structure to the Himalayan trend. The higher $D$ values in the Indo-Burma ranges (1.70–1.80) indicate clustering of epicentres in 2D space, due to greater stress concentration. The greater stress concentration may be due to bending of the subducting Indian plate as well as external forces due to overriding Burmese plate in this zone[17]; maximum interplay between the two plates causes more external forces for the higher $D$ values. In 1° mapping, the higher $D$ contours are most prominent along the Kopili Fault, the Shillong Plateau and the Indo-Burma ranges.

Since the data set is selected within 150 km distance of the permanent network, the Bengal basin and Tripura fold belt areas could not be examined or compared in this study. Sunmonu and Dimri[31], however, studied fractal dimension in these two tectonic blocks by box-counting method using the teleseismic ISC data ($M \geq 4.5$). They estimated $D$ value as 1.66 in the Tripura fold belt and 1.41 in the Bengal basin areas for the crustal earthquakes. Their results are comparable with the present study in this region.

The $b$-value and the fractal dimension mapping in NE India have identified the seismogenic structures along the Kopili Fault and the Indo-Burma ranges. The higher $D$ values along the Kopili Fault are due to the heterogeneous transverse structure. This observation suggests a higher risk zone along this fault. The higher $D$ values in the Indo-Burma ranges are due to greater stress concentration. The $b$-value maps clearly depict the variations of the earthquake frequency in the region; the higher $b$-value contours are comparable with the higher fractal dimension contours. The average value of '$b$' in NE India is found to be nearly 1.0. The spatial variation of this $b$ parameter is interpreted in terms of the different tectonic structure/domain of the region.


1. Gutenberg, R. and Richter, C. F., *Bull. Seismol. Soc. Am.*, 1954, **34**, 185–188.
2. Mogi, K., Bull. Earthquake Res. Inst., Univ. Tokyo, 1962, **40**, 831–853.
3. Scholtz, C. H., *Bull. Seismol. Soc. Am.*, 1968, **58**, 399–415.
4. Biswas, S. and Majumdar, R. K., *Geofizika*, 1988, **5**, 107–119.
5. Ma, H. C., *Acta Seismol. Sin.*, 1978, **21**, 126–141.
6. Smith, W. D., *Nature*, 1981, **289**, 136–139.
7. Majumdar, R. K. and Biswas, S., Proceedings of National Workshop on Disaster Management, Kolkata, 1999, vol. 1, pp. 73–85.
8. Omori, F. J., *Coll. Sci. Imp. Univ. Tokyo*, 1894, **7**, 111–200.
9. Kagan, Y. Y. and Knopoff, L., *Geophys. J.R. Astron. Soc.*, 1980, **62**, 303–320.
10. Mandelbrot, B. B., *The Fractal Geometry of Nature*, Freeman, San Francisco, 1982.
11. Aviles, C. A., Scholz, C. H. and Boatwright, J., *J. Geophys. Res.*, 1987, **92**, 331–344.
12. Hirata, T., *ibid*, 1989, **94**, 7507–7514.
13. Ogata, Y., *J. Am. Stat. Assoc.*, 1988, **83**, 9–27.
14. Shimazaki, T. and Nagahama, H., *Iwanami Shotten, Tokyo*, 1995, **65**, 241–256.
15. Aki, K., in *Earthquake Prediction*, Am. Geophys. Union, Washington DC, 1981, vol. 4, pp. 566–574.
16. Tosi, P., *Ann. Geofis.*, 1998, **41**, 215–224.
17. Kayal, J. R., *J. Himalayan Geol.*, 1996, **17**, 53–69.

18. Ni, J. and Barajangi, M., *Himalayan J. Geophys. Res.*, 1984, **89**, 1147–1163.
19. Kayal, J. R., De, Reena and Chakraborty, P., *Tectonophysics*, 1993, **218**, 375–381.
20. Mukhopadhyay, M. and Dasgupta, S., *ibid*, 1988, **149**, 299–322.
21. Kumar, M. R. and Rao, N. P., *Phys. Earth Planet. Inter.*, 1995, **90**, 75–80.
22. Biswas, S. and Majumdar, R. K., *Tectonophysics*, 1997, **269**, 323–336.
23. Kayal, J. R. and De, Reena, *Bull. Seismol. Soc. Am.*, 1991, **81**, 131–138.
24. Dasgupta, S. and Nandy, D. R., Proc. VII Symp. Earthquake Eng. Univ. Roorkee, 1982, vol. 1, pp. 19–24.
25. Ishikawa, Y., Statistical Methods for Detection of a Normal Precursory Phenomena in Geophysics, 1987, pp 124–142.
26. Smith, T. A., *Phys. Lett. A*, 1988, **133**, 283–288.
27. Grassberger, P. and Procaccia, I., *Physica D*, 1983, **9**, 189–208.
28. Aki, K., *Bull. Earthquake Res. Inst. Univ. Tokyo*, 1965, **43**, 237–239.
29. Idziak, A. and Teper, L., *Pure Appl. Geophys.*, 1996, **147**, 239–247.
30. Angulo-Brown, F., Ramirez-Guzman, A. H., Yepez, E., Rudoif-Navarro, A. and Pavia-Miller, C. G., *Geofis. Int.*, 1998, **37**, 29–33.
31. Sunmonu, A. and Dimri, V. P., *J. Geol. Soc. India*, 1999, **53**, 587–592.

ACKNOWLEDGEMENTS. We are grateful to Dr B. S. R. Murthy, Deputy Director General (Geophysics), GSI for his encouragement and kind support. The paper is published with the kind permission of the Director General, GSI. We thank the RRL(J) for the Bulletins and reviewers for their constructive comments to improve the manuscript.

Received 26 November 2001; revised accepted 26 March 2002